Area-Preserving Surface Parameterizations via Riemannian Optimization

Marco Sutti

Postdoctoral fellow at GSSI

Joint work with Mei-Heng Yueh

Mathematics of Data-Driven Models

January 28, 2026

Overview

Talk based on two papers:

- Riemannian gradient descent for spherical area-preserving mappings, M. Sutti and M.-H. Yueh, AIMS Math., Vol. 9(7), 19414–19445, 12 June 2024.
- Toroidal area-preserving parameterizations of genus-one closed surfaces, M. Sutti, M.-H. Yueh, Tech. report, to appear in Springer's Journal of Scientific Computing, 2026.

Main contributions:

(i) Combine tools from Riemannian optimization and computational geometry to propose a Riemannian optimizers for computing spherical (and toroidal) area-preserving mappings of genus-0 (resp., genus-1) closed surfaces.

(ii) Numerical experiments on several mesh models demonstrate the accuracy and efficiency of the algorithm.

(iii) Competitiveness and efficiency of our algorithm over three state-of-the-art methods for computing area-preserving mappings.

I. Simplicial surfaces and mappings, authalic and stretch energies

Simplicial surfaces and mappings/1

- A simplicial surface $\mathcal{M}$ is the underlying set of a simplicial 2-complex $\mathcal{K}(\mathcal{M}) = \mathcal{F}(\mathcal{M}) \cup \mathcal{E}(\mathcal{M}) \cup \mathcal{V}(\mathcal{M})$ composed of vertices

$$\mathcal{V}(\mathcal{M}) = \left\{ v_\ell = \left(v_\ell^1, v_\ell^2, v_\ell^2 \right)^\top \in \mathbb{R}^3 \right\}_{\ell=1}^{n},$$

oriented triangular faces

$$\mathcal{F}(\mathcal{M}) = \left\{ \tau_\ell = [v_{i_\ell}, v_{j_\ell}, v_{k_\ell}] \mid v_{i_\ell}, v_{j_\ell}, v_{k_\ell} \in \mathcal{V}(\mathcal{M}) \right\}_{\ell=1}^{m},$$

and undirected edges

$$\mathcal{E}(\mathcal{M}) = \left\{ [v_i, v_j] \mid [v_i, v_j, v_k] \in \mathcal{F}(\mathcal{M}) \text{ for some } v_k \in \mathcal{V}(\mathcal{M}) \right\}.$$

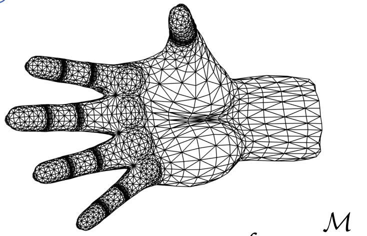

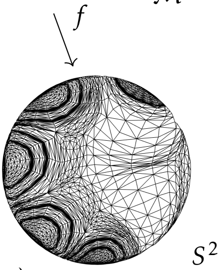

- A simplicial mapping $f : \mathcal{M} \to \mathbb{R}^3$ is a particular type of piecewise affine mapping with the restriction mapping $f|_\tau$ being affine, for every $\tau \in \mathcal{F}(\mathcal{M})$.

Simplicial surfaces and mappings/2

- We denote

$$\mathbf{f}_\ell := f(v_\ell) = \left(f_\ell^1, f_\ell^2, f_\ell^3\right)^\top,$$

  for every $v_\ell \in \mathcal{V}(\mathcal{M})$.

- The (image of the) mapping f can be represented as a matrix

$$\mathbf{f} = \begin{bmatrix} \mathbf{f}_1^\top \\ \vdots \\ \mathbf{f}_n^\top \end{bmatrix} = \begin{bmatrix} f_1^1 & f_1^2 & f_1^3 \\ \vdots & \vdots & \vdots \\ f_n^1 & f_n^2 & f_n^3 \end{bmatrix} =: \begin{bmatrix} \mathbf{f}^1 & \mathbf{f}^2 & \mathbf{f}^3 \end{bmatrix},$$

  or a vector

$$\operatorname{vec}(\mathbf{f}) = \begin{bmatrix} \mathbf{f}^1 \\ \mathbf{f}^2 \\ \mathbf{f}^3 \end{bmatrix}.$$

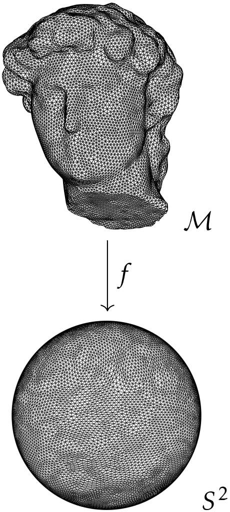

- A simplicial mapping $f : \mathcal{M} \to \mathbb{R}^3$ is said to be area-preserving if $|f(\tau)| = |\tau|$ for every $\tau \in \mathcal{F}(\mathcal{M})$.

Authalic energy

The authalic (or equiareal) energy for simplicial mappings $f : \mathcal{M} \to \mathbb{R}^3$ is

$$E_A(f) = E_S(f) - \mathcal{A}(f),$$

where $\mathcal{A}(f)$ is the image area, E_S is the stretch energy defined as

$$E_S(f) = \frac{1}{2}\,\mathrm{vec}(\mathbf{f})^\top (I_3 \otimes L_S(f))\,\mathrm{vec}(\mathbf{f}),$$

where $L_S(f)$ is the weighted Laplacian matrix $L_S(f)$, defined by

$$[L_S(f)]_{i,j} = \begin{cases} -\sum_{[v_i,v_j,v_k]\in\mathcal{F}(\mathcal{M})} [\omega_S(f)]_{i,j,k} & \text{if } [v_i,v_j]\in\mathcal{E}(\mathcal{M}), \\ -\sum_{\ell\neq i}[L_S(f)]_{i,\ell} & \text{if } j = i, \\ 0 & \text{otherwise,} \end{cases}$$

in which $\omega_S(f)$ is the modified cotangent weight defined as

$$[\omega_S(f)]_{i,j,k} = \frac{\cot(\theta_{i,j}^k(f))\,|f([v_i,v_j,v_k])|}{2|[v_i,v_j,v_k]|}.$$

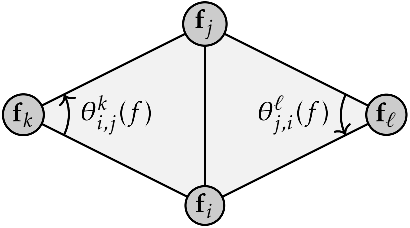

Stretch energy

- The stretch energy can be reformulated as [see Lemma 3.1, Yueh 2023]

$$E_S(f) = \sum_{\tau \in \mathcal{F}(\mathcal{M})} \frac{|f(\tau)|^2}{|\tau|}.$$

- (If the area-preserving simplicial mapping exists) then every minimizer of $E_S(f)$ is an area-preserving mapping and vice-versa [Thm. 3.3, Yueh 2023], i.e.,

$$f = \underset{|g(\mathcal{M})|=|\mathcal{M}|}{\operatorname{argmin}} E_S(g)$$

if and only if $|f(\tau)| = |\tau|$ for every $\tau \in \mathcal{F}(\mathcal{M})$.

- It is also proved that $E_A(f) \geqslant 0$ and the equality holds if and only if f is area-preserving [Cor. 3.4, Yueh 2023].

Theoretical foundation of the stretch energy minimization for area-preserving simplicial mappings: [Yueh 2023]

II. Riemannian optimization framework and geometry

Riemannian optimization

- The Riemannian optimization framework solves constrained optimization problems where the constraints have a geometric nature.
  - Exploit the underlying geometric structure of the problems. The optimization variables are constrained to a smooth manifold.

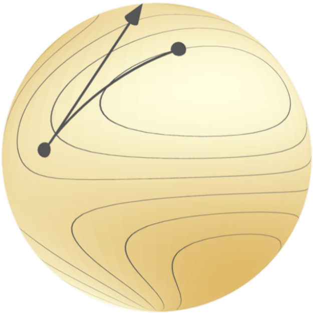

- In our setting: The problem is formulated on a power manifold of n unit spheres embedded in $\mathbb{R}^3$, and we use the RGD method for minimizing the cost function on this power manifold.
- Traditional optimization methods rely on the Euclidean space structure.
  - For instance, the steepest descent method for minimizing $g\colon \mathbb{R}^n \to \mathbb{R}$ updates $\mathbf{x}_k$ by moving in the direction $\mathbf{d}_k$ of the anti-gradient of g, by a step size α_k chosen according to an appropriate line-search rule.

Manifold optimization: [Edelman et al. 1998, Absil et al. 2008, Boumal 2023], …
The image above has been taken from the Manopt website: https://www.manopt.org/

Geometry of the unit sphere S^2

The unit sphere S^2 is a Riemannian submanifold of $\mathbb{R}^3$ defined as

$$S^2 = \{\mathbf{x} \in \mathbb{R}^3 : \mathbf{x}^\top \mathbf{x} = 1\}.$$

The Riemannian metric on the unit sphere is inherited from $\mathbb{R}^3$, i.e.,

$$\langle \boldsymbol{\xi}, \boldsymbol{\eta} \rangle_{\mathbf{x}} = \boldsymbol{\xi}^\top \boldsymbol{\eta}, \quad \boldsymbol{\xi}, \boldsymbol{\eta} \in \mathrm{T}_{\mathbf{x}} S^2,$$

where $\mathrm{T}_{\mathbf{x}} S^2$ is the tangent space to S^2 at $\mathbf{x} \in S^2$, defined as the set of all vectors orthogonal to $\mathbf{x}$ in $\mathbb{R}^3$, i.e.,

$$\mathrm{T}_{\mathbf{x}} S^2 = \{\mathbf{z} \in \mathbb{R}^3 : \mathbf{x}^\top \mathbf{z} = 0\}.$$

The projector $\mathrm{P}_{\mathrm{T}_{\mathbf{x}} S^2} : \mathbb{R}^3 \to \mathrm{T}_{\mathbf{x}} S^2$ is defined by

$$\mathrm{P}_{\mathrm{T}_{\mathbf{x}} S^2}(\mathbf{z}) = (I_3 - \mathbf{x}\mathbf{x}^\top)\,\mathbf{z}.$$

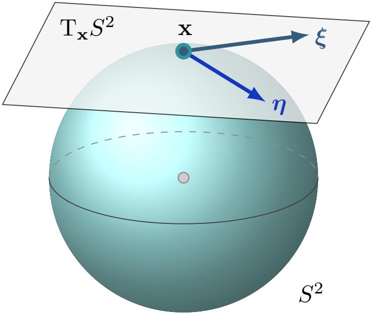

In the following, points on the unit sphere are denoted by $\mathbf{f}_\ell$ (the vertices of the simplicial mapping f), and tangent vectors are represented by $\boldsymbol{\xi}_\ell$.

Geometry of the power manifold $\left(S^2\right)^n$

We aim to minimize the function $E(f) = E(\mathbf{f}_1, \ldots, \mathbf{f}_n)$, where each $\mathbf{f}_\ell$, $\ell = 1, \ldots, n$, lives on the same manifold S^2.

$\rightsquigarrow$ This leads us to consider the power manifold of n unit spheres

$$\left(S^2\right)^n = \underbrace{S^2 \times S^2 \times \cdots S^2}_{n \text{ times}},$$

with the metric of S^2 extended elementwise.

In the next slides, we present the tools from Riemannian geometry needed to generalize gradient descent to this manifold, namely:

- The projector onto the tangent space to $\left(S^2\right)^n$ is used to compute the Riemannian gradient.
- The projection onto $\left(S^2\right)^n$ turns points of $\mathbb{R}^{n\times 3}$ into points of $\left(S^2\right)^n$.
- The retraction turns an objective function defined on $\mathbb{R}^{n\times 3}$ into an objective function defined on the manifold $\left(S^2\right)^n$.

Projector onto the tangent space to $\left(S^2\right)^n$

Here, the points are denoted by $\mathbf{f}_\ell \in \mathbb{R}^3$, $\ell = 1, \dots, n$, so we write

$$\mathrm{P}_{\mathrm{T}_{\mathbf{f}_\ell} S^2} = I_3 - \mathbf{f}_\ell \mathbf{f}_\ell^\top.$$

It clearly changes for every vertex $\mathbf{f}_\ell$. The projector from $\mathbb{R}^{n\times 3}$ onto the tangent space at $\mathbf{f}$ to the power manifold $\left(S^2\right)^n$ is a mapping

$$\mathrm{P}_{\mathrm{T}_{\mathbf{f}}\left(S^2\right)^n} \colon \mathbb{R}^{n\times 3} \to \mathrm{T}_{\mathbf{f}}\left(S^2\right)^n,$$

and can be represented by a block diagonal matrix of size $3n \times 3n$, i.e.,

$$\mathrm{P}_{\mathrm{T}_{\mathbf{f}}\left(S^2\right)^n} := \operatorname{blkdiag}\left(\mathrm{P}_{\mathrm{T}_{\mathbf{f}_1} S^2}, \mathrm{P}_{\mathrm{T}_{\mathbf{f}_2} S^2}, \dots, \mathrm{P}_{\mathrm{T}_{\mathbf{f}_n} S^2}\right) = \begin{bmatrix} \mathrm{P}_{\mathrm{T}_{\mathbf{f}_1} S^2} & & & \\ & \mathrm{P}_{\mathrm{T}_{\mathbf{f}_2} S^2} & & \\ & & \ddots & \\ & & & \mathrm{P}_{\mathrm{T}_{\mathbf{f}_n} S^2} \end{bmatrix}.$$

Projection onto the power manifold $\left(S^2\right)^n$

The projection of a single vertex $\mathbf{f}_\ell$ from $\mathbb{R}^3$ to the unit sphere S^2 is given by the normalization

$$\widetilde{\mathbf{f}}_\ell = \frac{\mathbf{f}_\ell}{\|\mathbf{f}_\ell\|_2}.$$

Hence, the projection of the whole of $\mathbf{f}$ onto the power manifold $\left(S^2\right)^n$ is given by

$$\mathrm{P}_{\left(S^2\right)^n} \colon \mathbb{R}^{n\times 3} \to \left(S^2\right)^n,$$

defined by

$$\mathbf{f} \mapsto \widetilde{\mathbf{f}} := \operatorname{diag}\left(\frac{1}{\|\mathbf{f}_1\|_2}, \frac{1}{\|\mathbf{f}_2\|_2}, \dots, \frac{1}{\|\mathbf{f}_n\|_2}\right)\begin{bmatrix}\mathbf{f}_1 & \mathbf{f}_2 & \cdots & \mathbf{f}_n\end{bmatrix}^\top.$$

This representative matrix is only shown for illustrative purposes; in the actual implementation, we use row-wise normalization of $\mathbf{f}$.

Retraction

- The retraction of a tangent vector $\boldsymbol{\xi}_\ell$ from $\mathrm{T}_{\mathbf{f}_\ell} S^2$ to S^2 is a mapping $\mathrm{R}_{\mathbf{f}_\ell} \colon \mathrm{T}_{\mathbf{f}_\ell} S^2 \to S^2$, defined by

$$\mathrm{R}_{\mathbf{f}_\ell}(\boldsymbol{\xi}_\ell) = \frac{\mathbf{f}_\ell + \boldsymbol{\xi}_\ell}{\|\mathbf{f}_\ell + \boldsymbol{\xi}_\ell\|}.$$

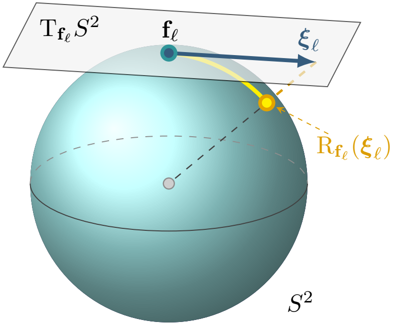

- For the power manifold $\left(S^2\right)^n$, the retraction of all the tangent vectors $\boldsymbol{\xi}_\ell$, $\ell = 1, \ldots, n$, is a mapping $\mathrm{R}_{\mathbf{f}} \colon \mathrm{T}_{\mathbf{f}}\left(S^2\right)^n \to \left(S^2\right)^n$, defined by

$$\begin{bmatrix} \boldsymbol{\xi}_1 & \cdots & \boldsymbol{\xi}_n \end{bmatrix}^\top \mapsto \operatorname{diag}\left(\frac{1}{\|\mathbf{f}_1 + \boldsymbol{\xi}_1\|_2}, \ldots, \frac{1}{\|\mathbf{f}_n + \boldsymbol{\xi}_n\|_2}\right) \begin{bmatrix} \mathbf{f}_1 + \boldsymbol{\xi}_1 & \cdots & \mathbf{f}_n + \boldsymbol{\xi}_n \end{bmatrix}^\top.$$

Constructing retractions: [Absil/Malick 2012]

Riemannian gradient descent method/1

- The Riemannian gradient of the objective function E is given by the projection onto $\mathrm{T}_{\mathbf{f}}\big(S^2\big)^n$ of the Euclidean gradient of E, namely,

$$\operatorname{grad} E(f) = \mathrm{P}_{\mathrm{T}_{\mathbf{f}}\left(S^2\right)^n}(\nabla E(f)).$$

- This is always the case for embedded submanifolds; see Prop. 3.6.1 in Absil et al., 2008.

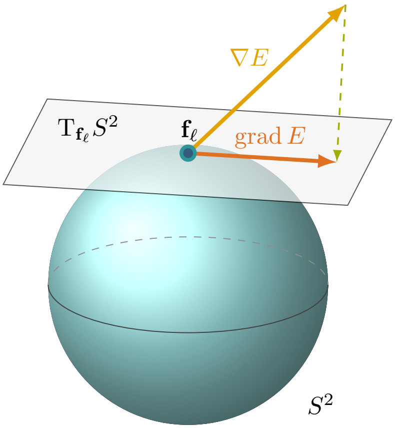

Riemannian gradient descent method/2

Algorithm 1: The RGD method on $\left(S^2\right)^n$.

Given objective function E, power manifold $\left(S^2\right)^n$, initial iterate$^{(*)}$ $\mathbf{f}^{(0)} \in \left(S^2\right)^n$, projector $\mathrm{P}_{\mathrm{T}_{\mathbf{f}}\left(S^2\right)^n}$ from $\mathbb{R}^{n\times 3}$ to $\mathrm{T}_{\mathbf{f}}\left(S^2\right)^n$, retraction $\mathrm{R}_{\mathbf{f}}$ from $\mathrm{T}_{\mathbf{f}}\left(S^2\right)^n$ to $\left(S^2\right)^n$;

Result: Sequence of iterates $\{f^{(k)}\}$.

$k \leftarrow 0$;

while *$f^{(k)}$ does not sufficiently minimizes E* **do**

- Compute the Euclidean gradient of the objective function $\nabla E(f^{(k)})$;
- Compute the Riemannian gradient as $\operatorname{grad} E(f^{(k)}) = \mathrm{P}_{\mathrm{T}_{\mathbf{f}^{(k)}}\left(S^2\right)^n}\left(\nabla E(f^{(k)})\right)$;
- Choose the anti-gradient direction $\mathbf{d}^{(k)} = -\operatorname{grad} E(f^{(k)})$;
- Use a line-search procedure to compute a step size $\alpha_k > 0$ that satisfies the sufficient decrease condition;
- Set $\mathbf{f}^{(k+1)} = \mathrm{R}_{\mathbf{f}^{(k)}}(\alpha_k \mathbf{d}^{(k)})$;
- $k \leftarrow k + 1$;

end while

$^{(*)}$ The initial mapping $\mathbf{f}^{(0)} \in \left(S^2\right)^n$ is computed via the fixed-point iteration (FPI) method of Yueh et al., 2019, until the first increase in energy is detected.

III. Numerical experiments

The benchmark triangular mesh models

Model Name	Right Hand	David Head	Cortical Surface	Bull
# Faces	8,808	21,338	30,000	34,504
# Vertices	4,406	10,671	15,002	17,254
			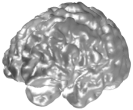	

Model Name	Bulldog	Lion Statue	Gargoyle	Max Planck
# Faces	99,590	100,000	100,000	102,212
# Vertices	49,797	50,002	50,002	51,108
				

Model Name	Bunny	Chess King	Art Statuette	Bimba
# Faces	111,364	263,712	895,274	1,005,146
# Vertices	55,684	131,858	447,639	502,575
			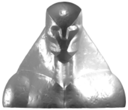	

Resulting spherical mappings

Comparison with other methods/1

Comparison with the fixed-point iteration method for minimizing the authalic energy E_A of Yueh et al., 2019.

	Fixed point method [Yueh et al. 19]			**Our RGD method**		
Model Name	SD/Mean	$E_A(f)$	Time	**SD/Mean**	$\boldsymbol{E_A(f)}$	**Time**
Right Hand	0.4598	2.92×10^0	1.35	**0.1204**	$\mathbf{9.40 \times 10^{-2}}$	**4.07**
David Head	0.0169	3.58×10^{-3}	4.30	**0.0156**	$\mathbf{3.04 \times 10^{-3}}$	**9.16**
Cortical Surface	0.0174	3.21×10^{-3}	5.62	**0.0200**	$\mathbf{3.72 \times 10^{-3}}$	**16.01**
Bull	0.1876	4.59×10^{-1}	6.90	**0.1348**	$\mathbf{2.19 \times 10^{-1}}$	**18.89**
Bulldog	0.1833	3.99×10^{-1}	22.22	**0.0343**	$\mathbf{1.27 \times 10^{-2}}$	**61.93**
Lion Statue	0.2064	5.28×10^{-1}	23.67	**0.1894**	$\mathbf{4.54 \times 10^{-1}}$	**76.76**
Gargoyle	4.1020	4.85×10^2	36.10	**0.0646**	$\mathbf{4.76 \times 10^{-2}}$	**80.52**
Max Planck	0.1844	1.67×10^1	25.99	**0.0525**	$\mathbf{3.39 \times 10^{-2}}$	**75.60**
Bunny	0.0394	3.96×10^{-2}	35.78	**0.0390**	$\mathbf{1.91 \times 10^{-2}}$	**89.62**
Chess King	1.0903	1.79×10^1	88.04	**0.0647**	$\mathbf{5.23 \times 10^{-2}}$	**207.47**
Art Statuette	0.0908	1.07×10^{-1}	342.95	**0.0405**	$\mathbf{2.10 \times 10^{-2}}$	**654.57**
Bimba Statue	0.0932	7.42×10^{-2}	305.00	**0.0512**	$\mathbf{3.29 \times 10^{-2}}$	**775.36**

Fixed-point iteration method for minimizing the authalic energy: [Yueh et al. 2019]

Comparison with other methods/2

Comparison with the adaptive area-preserving parameterization for genus-zero closed surfaces proposed by Choi et al., 2022.

	Choi et al., 2022			**Our RGD method**		
Model Name	SD/Mean	$E_A(f)$	Time	**SD/Mean**	$\boldsymbol{E_A(f)}$	**Time**
Right Hand	18.3283	4.84×10^{3}	218.03	**0.1204**	$\mathbf{9.40\times10^{-2}}$	**4.07**
David Head	0.0426	2.27×10^{-2}	298.76	**0.0156**	$\mathbf{3.04\times10^{-3}}$	**9.16**
Cortical Surface	0.6320	1.14×10^{0}	420.20	**0.0200**	$\mathbf{3.72\times10^{-3}}$	**16.01**
Bull	8.5565	1.82×10^{3}	34.42	**0.1348**	$\mathbf{2.19\times10^{-1}}$	**18.89**
Bulldog	9.2379	1.22×10^{3}	183.94	**0.0343**	$\mathbf{1.27\times10^{-2}}$	**61.93**
Lion Statue	0.2626	8.96×10^{-1}	1498.91	**0.1894**	$\mathbf{4.54\times10^{-1}}$	**76.76**
Gargoyle	0.3558	1.30×10^{0}	1483.35	**0.0646**	$\mathbf{4.76\times10^{-2}}$	**80.52**
Max Planck	11.6875	1.49×10^{3}	195.39	**0.0525**	$\mathbf{3.39\times10^{-2}}$	**75.60**
Bunny	27.6014	8.94×10^{3}	157.87	**0.0390**	$\mathbf{1.91\times10^{-2}}$	**89.62**
Chess King	11.8300	1.65×10^{3}	608.55	**0.0647**	$\mathbf{5.23\times10^{-2}}$	**207.47**
Art Statuette	394.4414	9.93×10^{0}	2284.79	**0.0405**	$\mathbf{2.10\times10^{-2}}$	**654.57**
Bimba Statue	0.5110	2.01×10^{0}	16 773.34	**0.0512**	$\mathbf{3.29\times10^{-2}}$	**775.36**

Adaptive area-preserving parameterization for genus-zero closed surfaces: [Choi/Giri/Kumar 2022]

Texture mapping

- Texture mapping: computer graphics technique for applying 2D images to 3D models.

(a) (b) (c)

(a) (b) (c)

Applications from the paper: Toroidal area-preserving parameterizations of genus-one closed surfaces, M. Sutti, M.-H. Yueh, Tech. report, to appear in Springer's Journal of Scientific Computing, 2026.

Surface registration

- A registration mapping between surfaces $\mathcal{M}_0$ and $\mathcal{M}_1$ is a bijective mapping $g\colon \mathcal{M}_0 \to \mathcal{M}_1$. An ideal registration mapping keeps important landmarks aligned while preserving specified geometry properties.
- Framework for the computation of landmark-aligned area-preserving parameterizations of genus-zero closed surfaces.
- Illustration with the landmark-aligned morphing process from one brain to another.

Problem statement: Given a set of landmark pairs (in this case, four sulci) $\{(p_i, q_i) \mid p_i \in \mathcal{M}_0,\ q_i \in \mathcal{M}_1\}_{i=1}^{m}$, our goal is to compute an area-preserving simplicial mapping $g\colon \mathcal{M}_0 \to \mathcal{M}_1$ that satisfies $g(p_i) \approx q_i$, for $i = 1, \ldots, m$.

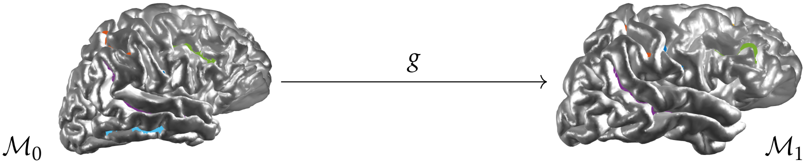

Brain and vertebrae morphing

- Brain and vertebrae morphing via the linear homotopy method.
- A landmark-aligned morphing process from $\mathcal{M}_0$ to $\mathcal{M}_1$ can be constructed by the linear homotopy $H\colon \mathcal{M}_0 \times [0,1] \to \mathbb{R}^3$ defined as

$$H(v,t) = (1-t)\,v + t\,g(v).$$

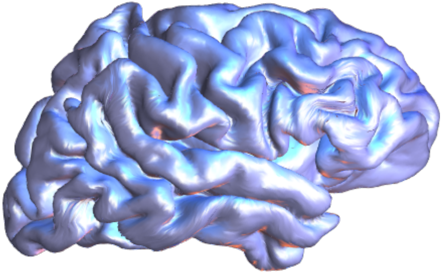

Conclusions

Main contributions:

- Riemannian optimization & computational geometry $\rightsquigarrow$ RGD and other methods for computing spherical area-preserving mappings of genus-zero closed surfaces.
- Extensive numerical experiments on various mesh models to demonstrate the algorithm's stability and effectiveness.
- Texture mapping.
- Landmark-aligned surface registration between two human brain models, and between two vertebrae.

Thank you for your attention!